Neurochemistry International 78 (2014) 79–87

Contents lists available at ScienceDirect

Neurochemistry International

journal homepage: www.elsevier.com/locate/nci

Further evidence for the neuroprotective role of oleanolic acid in a model of focal brain hypoxia in rats

Laura Caltana [a,*], Damián Rutolo [a], María Luisa Nieto [b], Alicia Brusco [a]

[a] Instituto de Biología Celular y Neurociencia, IBCN (UBA-CONICET), Buenos Aires, Argentina
[b] Instituto de Biología y Genética Molecular, CSIC-UVA, Valladolid, Spain

ARTICLE INFO

Article history:
Received 7 April 2014
Received in revised form 15 September 2014
Accepted 25 September 2014
Available online 2 October 2014

Keywords:
Oleanolic acid
Hypoxia
Neuronal death
Brain injury
Neuroprotection

ABSTRACT

Ischemic brain injury is a dynamic process involving oxidative stress, inflammation, cell death and the activation of endogenous adaptive and regenerative mechanisms depending on the activation of transcription factors such as hypoxia-inducible factor 1-alpha. Accordingly, we have previously described a new focal hypoxia model by direct intracerebral cobalt chloride injection. In turn, oleanolic acid, a plant-derived triterpenoid, has been extensively used in Asian countries for its anti-inflammatory and anti-tumor properties. A variety of novel pharmacological effects have been attributed to this triterpenoid, including beneficial effects on neurodegenerative disorders – including experimental autoimmune encephalomyelitis – due to its immunomodulatory activities at systemic level, as well as within the central nervous system. In this context, we hypothesize that this triterpenoid may be capable of exerting neuroprotective effects in ischemic brain, suppressing glial activities that contribute to neurotoxicity while promoting those that support neuronal survival. In order to test this hypothesis, we used the intraperitoneal administration of oleanoic acid in adult rats for seven days previous to focal cortical hypoxia induced by cobalt chloride brain injection. We analyzed the neuroprotective effect of oleanoic acid from a morphological point of view, focusing on neuronal survival and glial reaction.

1. Introduction

Traditional medicines and phytopharmaceutical compounds have both been used for the treatment of inflammatory and degenerative diseases. For example, the Mediterranean diet, whose health benefits have long been attributed to a high content of monounsaturated fatty acids and in which olive oil is the major source of dietary fat intake, has been associated with low incidence of cardiovascular diseases (Chiva-Blanch et al., 2014; Delgado-Lista et al., 2014) and cancer (Bao et al., 2014; Villar et al., 2014).

Terpenes in general, and triterpenes in particular, show anti-inflammatory activity and act as immunomodulators in nutraceutical agents. In particular, oleanolic acid (OA) (3b-hydroxy-olea-12-en-28-oic acid), a pentacyclic triterpene, is a natural compound found in various plants, fruits and herbs, and it is isolated from chloroform extract of *Olea ferruginea Royle* after the removal of organic bases and free acids (Sultana and Saify, 2012).

Several studies have been shown promising effects including anti-neoplastic (Srivastava et al., 2010), gastroprotective (Rodriguez et al., 2003), antibacterial (Fontanay et al., 2008) and anti-inflammatory (Lee et al., 2013). Neuroprotective effects were also described for OA in models of degenerative disease. OA suppreses NF-κB p65, Bax and cleaved caspase-3 production, and retains Bcl-2 expression (Tsai and Yin, 2012). In inflammatory demyelinating diseases like multiple sclerosis and its animal model, experimental autoimmune encephalomyelitis (EAE), the OA protected against EAE by restricting infiltration of inflammatory cells into the central nervous system (CNS) and by preventing blood–brain barrier disruption (Martin et al., 2012).

Often a result of ischemic stroke, hypoxia is defined as a situation in which O_2 supply is insufficient for normal metabolism, which produces a reduction in aerobic metabolism, loss of cellular function and eventual cell death (Ratan et al., 2007). With an approximate global incidence of 250–400 in 100,000 and a mortality rate of around 30%, stroke is the third most common cause of mortality and one of the leading causes of long-term disability (Lloyd-Jones et al., 2010). According to the World Health Organization, 15 million people suffer stroke worldwide every year, out of whom 5 million

Abbreviations: $CoCl_2$, cobalt chloride; OA, oleanolic acid; CNS, central nervous system; EAE, experimental autoimmune encephalomyelitis; SS, saline solution; i.p, intraperitoneal; PB, phosphate buffer; PBS, phosphate-buffered saline; GFAP, glial fibrillary acidic protein; MAP-2, microtubule-associated protein-2; iNOS, inducible nitric oxide synthase; VIM, vimentin; NADPH-D, nicotinamide adenine dinucleotide phosphate diaphorase.

* Corresponding author. Paraguay 2155, 3° Piso. Instituto de Biología Celular y Neurociencia "Prof. E. De Robertis" (UBA-CONICET). Facultad de Medicina. Universidad de Buenos Aires. Ciudad Autónoma de Buenos Aires (1121), Argentina. Tel.: +54 5950 9626.
E-mail address: lauracaltana@gmail.com (L. Caltana).

http://dx.doi.org/10.1016/j.neuint.2014.09.011
0197-0186/

die and another 5 million are permanently disabled (Mackay and Mensah, 2004). Although there are currently no effective treatments to enhance functional recovery following stroke, which is why it poses a massive socio-economic burden worldwide (Kunz et al., 2010), *in vitro* and *in vivo* models of hypoxia have shown neuroprotective effects against ischemic injury conferred by novel tritepenoid compound (Zhang et al., 2012).

We have previously used a hypoxia model, consisting in an intracortical injection of $CoCl_2$, which is widely used to induce hypoxic conditions both *in vivo* and *in vitro* (Karovic et al., 2007). Cobalt inactivates HIF-specific proline-hydroxylases (Berra et al., 2006; Epstein et al. 2001), impairing the binding of von Hippel–Lindau protein with HIF-1α (Yuan et al., 2003), causing the stabilization of HIF-1α and preventing its degradation by the proteasome. This in turn produces a focal hypoxia-like lesion by stabilizing and inducing HIF-1a and exhibiting neuronal and glial alterations (Caltana et al., 2009).

On the basis of the apparent protective effects of the Mediterranean diet against cardiovascular diseases, its high concentration of triterpenes such as oleanolic acid, and previous reports where the pretreatment with triterpenes protected the heart against myocardial infarction (Janahmadi et al., 2014), the aim of this work was to analyze the potential neuroprotective effect of OA pre-treatment (as a tool to prevent or attenuate the consequences) in a model of focal cerebral chemical hypoxia, focusing on neuronal survival and glial reaction.

2. Materials and methods

2.1. Animal treatment

Animal care for this experimental protocol was in accordance with the NIH guidelines for the Care and Use of Laboratory Animals and the principles presented by the Society for Neuroscience in the Guidelines for the Use of Animals in Neuroscience Research, and authorized by the CICUAL (Comité Institucional de Cuidado y Uso de Animales de Experimentación, School of Medicine, University of Buenos Aires). All efforts were made to reduce suffering and the number of animals used.

Sixteen adult male Wistar rats (250–300 g) obtained from the animal facility in the School of Pharmacy and Biochemistry, University of Buenos Aires, were used in this study. Rats were housed in a controlled environment (12 h/12 h light/dark cycle, controlled humidity and temperature, free access to standard laboratory rat food and water).

First, rats were divided into two groups –OA and SS–, which received, from day 1 to day 7, an intraperitoneal (i.p.) injection of either OA (6 mg/kg/day dissolved in DMSO and saline solution) or vehicle (DMSO dissolved in an equivalent volume of saline solution), respectively. Each group was in turn divided in two subgroups –$CoCl_2$ and SS– which received, on day 8 and at intracortical level, a surgically administered injection of either a solution of 50 mM cobalt chloride ($CoCl_2$) or saline solution (Caltana et al., 2009), respectively. Briefly, animals were subjected to a unilateral lesion by placing them in a stereotaxic apparatus and drilling a small hole on the skull in the frontoparietal cortex at Bregma -1.30 mm (Paxinos and Watson, 2013). Once the underlying pia was reached, a Hamilton syringe was used to inject sterile solution of $CoCl_2$ (50 mM) or saline solution in the right hemisphere, 1 mm below the pia level in the cerebral cortex (layers 3–4). The $CoCl_2$ solution was prepared in sterile-diluted saline solution adjusted to reach a physiological osmolarity of 310 mOsm/kg soon after the $CoCl_2$ was added. Then, the incision in the overlying skin was closed using the temporal muscle and the attached fascia to cover the lesion site. During surgery and the whole emergence period, animals' body temperature was maintained by means of a heating pad. Surgical procedures were performed under anesthesia induced with sevofluorane 8% (v/v) and each animal was later put in a separate cage for recovery. For two more days following surgical procedures, rats continued receiving OA or SS.

Experimental groups were thus as follows:

Control groups:

Group 1: SS-SS: intracerebrally injected with saline and pretreated with vehicle.
Group 2: SS-OA: intracerebrally injected with saline and pretreated with OA.

Hypoxic groups:

Group 3: $CoCl_2$-SS: intracerebrally injected with $CoCl_2$ and pretreated with vehicle.
Group 4: $CoCl_2$-OA: intracerebrally injected with $CoCl_2$ and pretreated with OA.

On the 11th day each animal was deeply anesthetized with sevofluorane 8% (v/v) and perfused through the left ventricle, initially with saline solution added to 50 IU heparin and 0.05% (w/v) $NaNO_2$, and subsequently with a fixative solution containing 4% (w/v) paraformaldehyde and 0.25% (v/v) glutaraldehyde in 0.1 M phosphate buffer, pH 7.2 (PB). Brains were removed and postfixed in the same cold fixative solution for 2 h. Brains were then washed three times in cold 0.1 M phosphate buffer, pH 7.4, containing 5% (w/v) sucrose, and left in the same washing solution for 18 h at 4 °C. Finally, brains were cryoprotected by immersion in a solution containing 25% (w/v) sucrose in PB and stored at –20 °C until used. Coronal 40-μm-thick brain sections corresponding to the area of saline and $CoCl_2$ injection sites were obtained using a cryostat and mounted on gelatin-coated slides.

2.2. Fluoro-Jade® B staining procedure

Brain sections were mounted with distilled water onto gelatin-coated slides and dried on a slide warmer at 50 °C for at least half an hour. Sections were then immersed in a solution containing 1% (w/v) sodium hydroxide in 80% alcohol for 5 minutes, followed by 2 minutes in 70% (v/v) alcohol and 2 minutes in distilled water. The slides were then transferred to a solution of 0.06% (w/v) potassium permanganate for 10 minutes. Slides were rinsed for 2 minutes in distilled water and then transferred to the Fluoro-Jade® B: 0.0004% staining solution for 20 minutes. After staining, sections were rinsed three times in distilled water. Excess water was drained off and slides were rapidly set at approximately 50 °C, until they were fully dry. Once dry, slides were immersed in xylene and then coverslipped using Permount mounting media. Sections were examined with an epifluorescence microscope using a filter system suitable for fluorescein or FITC visualization (Balan et al., 2006).

2.3. Immunohistochemistry

Cryostat brain sections of animals belonging to the different experimental groups were simultaneously processed as previously described (Evrard et al., 2006). Briefly, after phosphate-buffered saline (PBS) rinses, endogenous peroxidase activity was inhibited with 0.5% (v/v) H_2O_2 in PBS for 30 minutes at room temperature. Brain sections were then blocked for 1 hour with 3% (v/v) normal goat serum in PBS. After rinsing in PBS, sections were incubated for 48 hours at 4 °C with the primary antibodies and then rinsed and incubated 1 hour at room temperature with biotinylated secondary antibodies (1:400). After further washing in PBS, sections were incubated for 1 hour with the Extravidin complex solution (1:400).

After washing five times in PBS and twice in an 0.1 M acetate buffer, pH 6, the development of peroxidase activity was carried out with 0.035% (w/v) 3.3′-diaminobenzidine plus 2.5% (w/v) nickel ammonium sulfate and 0.1% (v/v) H_2O_2 dissolved in acetate buffer. After enzymatic incubation, sections were washed with distilled water, dehydrated and coverslipped using Permount.

All antibodies, as well as the Extravidin complex, were dissolved in PBS containing 1% (v/v) normal goat serum and 0.3% (v/v) Triton X-100, pH 7.4. Primary antibody dilutions were 1:3000 (glial fibrillary acidic protein, GFAP, Dako), 1:400 (inducible nitric oxide synthase, iNOS, Sigma), 1:1000 (microtubular associated protein-2, MAP2, Sigma), 1:800 (PAN, Abcam), 1:800 (S-100b protein, Sigma), 1:500 (Vimentin, VIM, Sigma).

Controls for the immunohistochemistry procedure were routinely performed by omitting the primary antibody. These control sections did not develop any immunohistochemical labeling.

2.4. Lectin staining

Sections were rinsed in PBS and endogenous peroxidase activity was inhibited with 0.5% (v/v) H_2O_2 for 30 minutes at room temperature. Brain sections were blocked for 1 hour with 3% (v/v) normal goat serum in PBS. After rinsing in PBS, sections were incubated for 48 hours at 4 °C with the biotynilated lectin (Ignácio et al., 2005) and then rinsed and incubated 1 hour with the Extravidin complex solution. After washing five times in PBS and twice in an 0.1 M acetate buffer, pH 6, the development of peroxidase activity was carried out with 0.035% (w/v) 3.3′-diaminobenzidine plus 2.5% (w/v) nickel ammonium sulfate and 0.1% (v/v) H_2O_2 dissolved in acetate buffer. After enzymatic incubation, sections were washed with distilled water, dehydrated and coverslipped using Permount. The dilutions of the L. esculentum lectin were used at 6 μg/ml (Sigma). Controls for the lectin staining procedure were routinely performed by omitting the lectin. These control sections did not develop labeling.

2.5. Nicotinamide-adenine dinucleotide phosphate-diaphorase (NADPH-d)

Tissue was processed with the NADPH-d histochemical method, following Scherer-Singler et al. (1983), which reveals the neurons that synthesize NO. Briefly, free floating sections were incubated for 1 h at 37 °C in a solution containing 0.1% β-NADPH (1 mg/ml) and 0.02% (0.2 mg/ml) nitro blue tetrazolium chloride diluted in 0.1 M phosphate buffer, pH 7.4, with 0.3% Triton X-100 (all reagents from Sigma). Negative controls were obtained by incubating floating sections in a reaction mixture without β-NADPH. Sections were mounted on gelatin-coated glass slides and coverslipped with Permount.

2.6. Morphometric analysis of digital images

Measurements of both groups of control and treated sections were carried out in standardized conditions (at the same session, in the same day). In each tissue section, each microscopic field was selected within the limits of the anatomical area of interest, the penumbra (for a description, see Caltana et al., 2009), to be morphometrically analyzed. Tissue images were obtained through an Axiolab Zeiss light microscope equipped with an Olympus Q-Color 3 cooled digital camera. Counting and morphometry were performed using Image Pro PLUS 4.5 (Media Cybernetics, Warrendale, PA, USA) and Image J (NIH, http://rsb.info.nih.gov/ij/) software.

As an indirect measurement of the concentration of S-100b in astrocytes and NOS in nervous cells, the intensity of the S-100b protein and iNOS immunostaining and NADPH-d staining were evaluated by means of a relative optical density (ROD) value, in respective cells. As previously described (Evrard et al., 2006), ROD values were obtained after the transformation of each mean gray value using the following formula: ROD = log (256/mean gray). In order to rule out local background ROD, a background parameter was obtained from each section out of the immunolabeled structures and subtracted from each cell ROD value before statistically processing the values obtained. ROD values are expressed as ROD units.

The number of Fluoro-Jade® B+ cells, VIM+ cells, and lectin+ cells were counted in a microscopic field of 1 mm^2.

For astrocytes (GFAP+ cells), we evaluated the individual cell area.

In order to evaluate the PAN+ and MAP2+ fibers, the total area of the immunolabeled fibers was related to the total area of the corresponding microscopic field (20× primary magnification), thus rendering a relative area parameter.

Three separate immunohistochemical experiments were run for each immunostaining study. Individual experiments were composed of 6 to 10 tissue sections of each animal from each group. Five to ten fields were measured from each brain area in each section of each animal by stereological analysis. Inter-animal differences in each of the four groups, as well as inter-experiment differences, were statistically non-significant. Reported values represent the mean ± SEM of experiments performed for each marker.

2.7. Statistical analysis

Differences among the means of the four groups were statistically analyzed by one-way analysis of variance (ANOVA). Tukey's multiple comparison test was conducted following the significance/non-significance of overall ANOVA. For Fluorajade+ cells, a *t*-test was performed. Statistical significance was set at $p < 0.05$. Statistical analyses were carried by means of GraphPad Prism v5.00 software (GraphPad Software Inc.). For graphic simplification, some values of the different groups are expressed as percentages of SS-SS values (100%).

3. Results

3.1. OA pre-treatment prevented hypoxia-induced neuronal degeneration and cytoskeleton changes in neurons

After $CoCl_2$ intracortical injection, the number of degenerated neurons (Fluoro-Jade® B+) was lower in $CoCl_2$-OA animals than in the $CoCl_2$-SS group, while neither the SS-OA nor the SS-SS showed degenerated neurons (Fig. 1).

In this study, the neuronal cytoskeleton was analyzed by two parameters: the dendritic tree, labeled with MAP2, and the axons, labeled with neurofilament marker PAN. The area analyzed was the penumbra region of the primary and secondary motor cortex (M1/M2), where the intracortical injection was administered.

MAP2 is a microtubule-associated protein shown in dendrites and cell bodies, used as a specific marker to analyze the dendritic tree and its extension. In our analysis of the area covered by MAP2+ fibers, non-hypoxic groups (SS-SS and SS-OA) showed equivalent expression patterns. The $CoCl_2$-SS group experimented a decrease in this parameter, while the other groups did not show changes (Fig. 2). In the $CoCl_2$-OA group, the area covered by MAP2+ dendrites reached values similar to those observed in the control groups.

PAN-labeled axonal prolongations showed a pattern similar to MAP2+ dendrites, with the $CoCl_2$-SS group exhibiting a lower number of PAN+ fibers than the other groups (Fig. 3).

The ROD of NADPH-d (used as a parameter of neuronal nitric oxide synthase, nNOS, activity) showed an increase after $CoCl_2$ injection with a decreasing tendency in OA treatment, although statistically non-significant (Fig. 4).

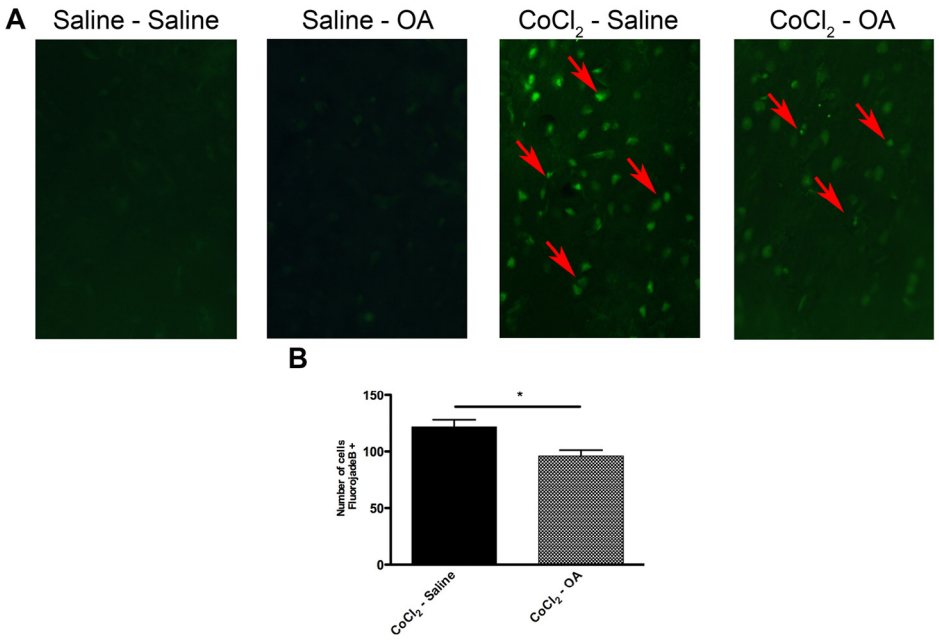

Fig. 1. A. Fotomicrography of Fluoro-Jade® B staining. Primary magnification 20×. B. Number of Fluoro-Jade® B + cells/mm^2. The groups SS-SS and SS-OA did not show Fluoro-Jade® B+ cells. Significance between treatments after one-way ANOVA and Tukey's post-test. * $p < 0.05$. Red arrows show Fluoro-Jade® B+ cells.

3.2. OA pre-treatment reduced astroglial reaction

Astroglial reaction was analyzed by measuring GFAP, the main astrocytic intermediate filament, and studying changes in each GFAP+ astrocytic area. No changes were observed in the astrocytic area, shape or organization pattern in the control groups, SS-SS or SS-OA (Fig. 5). In turn, the astrocytic area increased after chemical hypoxia in the $CoCl_2$-SS group, but exhibited no changes in the $CoCl_2$-OA group.

In addition, VIM, an intermediate filament of immature astrocytes, was used to determine the number of VIM+ cells. Results revealed a decrease after chemical hypoxia, which remained at normal levels in the $CoCl_2$-OA group (Fig. 6).

Finally, S-100b protein immunostaining was used to label the cell body and some of the primary astrocytic cytoplasmic projections and S-100b ROD was measured. Results showed no significant S100b ROD differences in control groups, while $CoCl_2$-SS rats showed a decrease in S100b ROD that was not observed in the $CoCl_2$-OA group (Fig. 7).

3.3. OA prevented microglial reaction

The extent of microglial activation was assessed by determining the number of lectin+ cells. No differences were found between the SS-OA and the SS-SS groups, with microglial cells typically ramified with multiple branches. In contrast, a robust microglial response

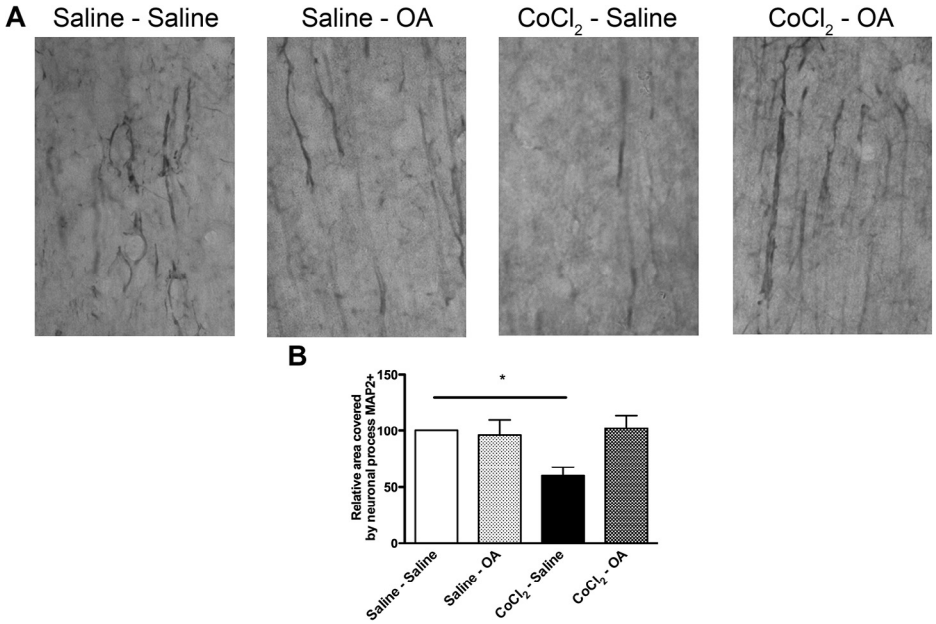

Fig. 2. A. Fotomicrography of MAP2 immunostaining. Primary magnification 20×. B. Relative area covered by MAP2+ fibers. Significance between treatments after one-way ANOVA and Tukey's post-test. * $p < 0.05$.

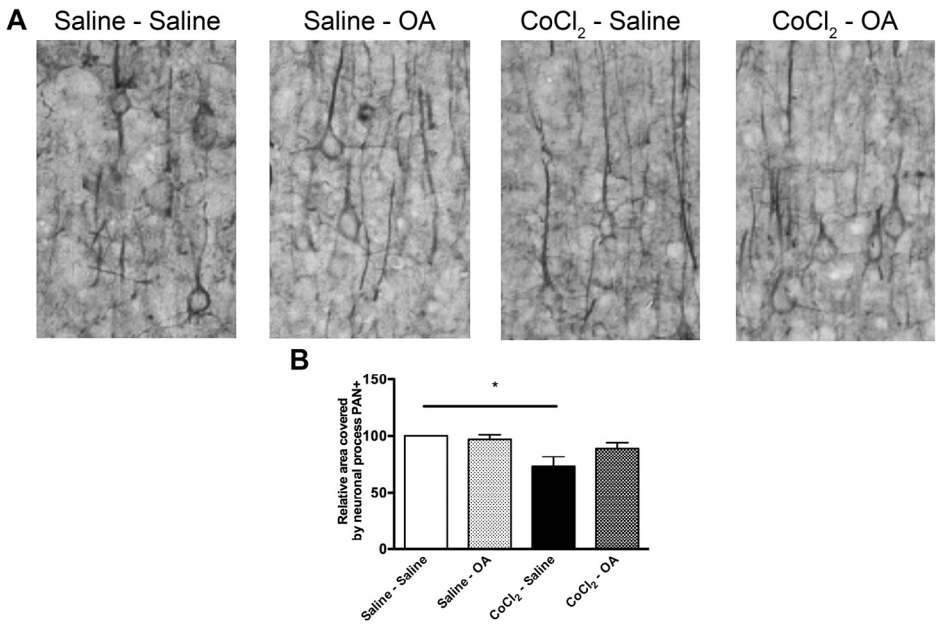

Fig. 3. A. Fotomicrography of PAN immunostaining. Primary magnification 20×. B. Relative area covered by PAN+ fibers. Significance between treatments after one-way ANOVA and Tukey's post-test. * $p < 0.05$.

was noted after $CoCl_2$ injection, as evidenced by a significant increase in the number of lectin+ cells (Fig. 8). Lower microglial activation was observed in the $CoCl_2$-OA group, although a comparison with the control group rendered it non-significant. In turn, no significant changes were found in iNOS ROD, except for an increasing tendency in the $CoCl_2$-SS group (Fig. 9).

4. Discussion

OA is a ubiquitous triterpenoid in the plant kingdom and an integral part of the human diet. During the last decade, it has been the focus of over 700 research articles, which reflects increasing interest and progress in the understanding of its properties. In this context, this study was designed to further ascertain the neuroprotective properties of OA after cerebral chemical hypoxia.

OA is relatively non-toxic and has been used in cosmetics and health products. Bibliographical evidence proves that the oral administration of OA is not as effective in inhibiting inflammatory reactions as i.p. or subcutaneous (s.c.) injections. Singh et al. observed no mortality during a 5-day period following a single s.c. injection of OA (1.0 g/kg) in mice or rats (Singh et al., 1992). In turn, the multiple administration of OA (180 mg/kg, orally) for 10 days

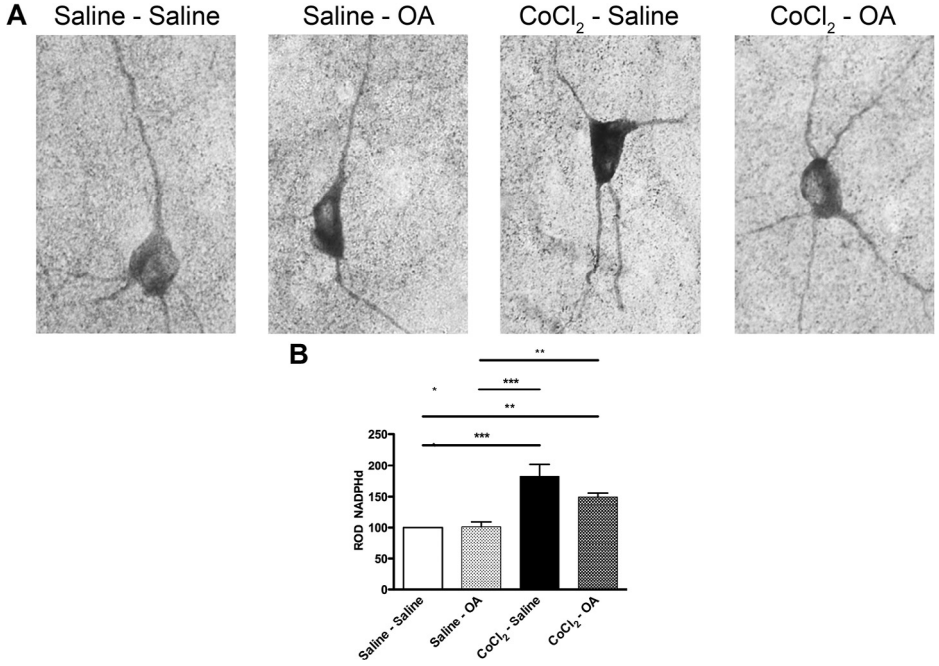

Fig. 4. A. Fotomicrography of NADPH-d staining. Primary magnification 40×. B. ROD of NADPH-d. Significance between treatments after one-way ANOVA and Tukey's post-test. * $p < 0.05$; ** $p < 0.01$; *** $p < 0.001$.

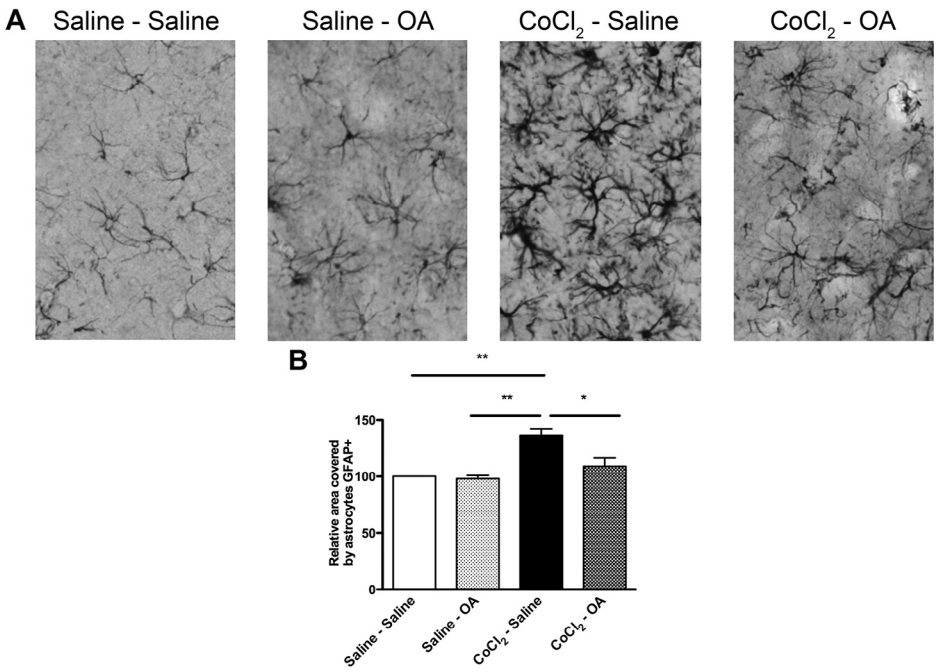

Fig. 5. A. Fotomicrography of GFAP immunostaining. Primary magnification 20×. B. Area covered by GFAP+ astrocytes. Significance between treatments after one-way ANOVA and Tukey's post-test. * $p < 0.05$; ** $p < 0.01$.

has proven not to generate abnormalities in the brain, heart, lung, liver, kidney, thyroid, testes, stomach, spleen or intestine (Hunan Med. Inst., 1977). In addition, at a dose of 50 mg/kg/day, s.c. triterpenes including OA, erythrodiol and uvaol have been proven safe and protective against inflammatory and degenerative diseases. In this study, we used an i.p. 6 mg/kg/day dose of OA, which is within the range (5–25 mg/kg/day) in which triterpenes are reported to be effective in brain-related disorders (Rong et al., 2011; Sarkar et al., 2014), and we show a decrease in neuronal degeneration and glial reaction. The neuroprotective effects of OA are evidenced by a reduction in Fluoro-Jade® B + cells and a recovery in dendritic and axonal extension, in agreement with other examples of the use of agents in ischemic injuries (Ramos et al., 2004).

During hypoxia, the generated free radicals damage DNA, proteins and lipids, thus producing neuronal death. nNOS and iNOS induce neuronal damage following hypoxia (Moro et al., 2004), while nitric oxide generated by high S-100b protein induces apoptosis in astrocytes (Hu and Van Eldik, 1996) and neurons *in vitro* (Hu et al., 1997). In our work, NADPH-d activity, which reflects nNOS

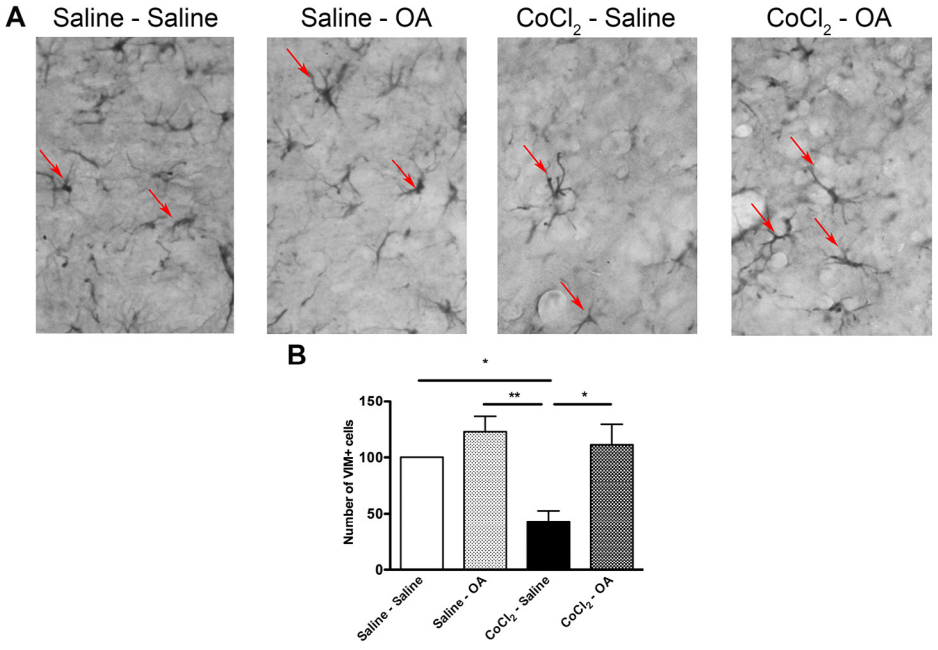

Fig. 6. A. Fotomicrography of VIM immunostaining. Primary magnification 20×. B. Number of VIM+ cells/mm^2. Significance between treatments after one-way ANOVA and Tukey's post-test. * $p < 0.05$; ** $p < 0.01$. Red arrows show VIM+ cells.

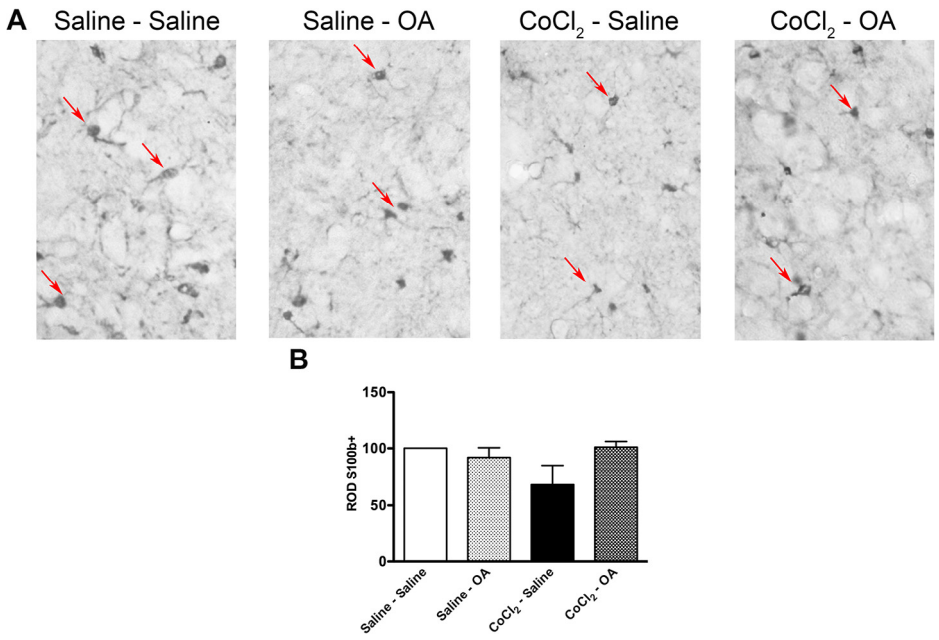

Fig. 7. A. Fotomicrography of S-100b protein immunostaining. Primary magnification 20×. B. ROD of S-100b protein. Significance between treatments after one-way ANOVA and Tukey's post-test. Red arrows show S100b+ cells.

activity, increased after $CoCl_2$ injection and showed a decreasing tendency in the OA pre-treated group.

OA reduced the GFAP+ astrocytic area and the number of VIM+ cells (Evrard et al., 2006), showing a decrease in astrogliosis.

Regarding the astrocytic response, it has been established that S-100b protein affects astrocytes in an autocrine manner and stimulates astrocyte cell line proliferation at low doses (Selinfreund et al., 1991). In our work, S-100b protein had no changes in any of the groups studied; however, when considering the relation between its expression and astrocytic reaction, and the increase in VIM+ cells in the OA pre-treated group, an increase was determined in $CoCl_2$-OA animals. S100-b protein exerts neurotrophic effects on neurons, stimulating neurite outgrowth and regeneration *in vitro* and *in vivo*, and enhancing neuronal survival after injury (Nardin et al., 2007). The protective effects of S-100b on neurons may also be indirect, with this protein stimulating the uptake of neurotoxic glutamate by astrocytes, and thus reducing the neurotoxin-dependent activation of microglia and astrocytes (Tramontina et al., 2006). In this way, S100-b protein might contribute to reduce the number of activated astrocytes during the course of brain injury and play a role in the process of resolution of inflammation.

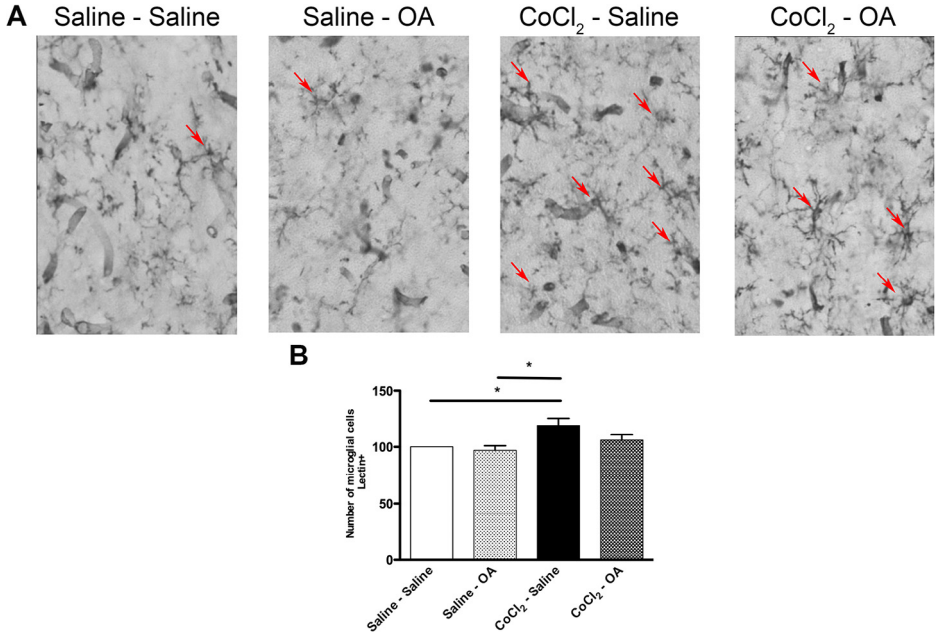

Fig. 8. A. Fotomicrography of lectin staining. Primary magnification 20×. B. Number of lectin+ cells/mm^2. Significance between treatments after one-way ANOVA and Tukey's post-test. * $p < 0.05$. Red arrows show lectin+ cells.

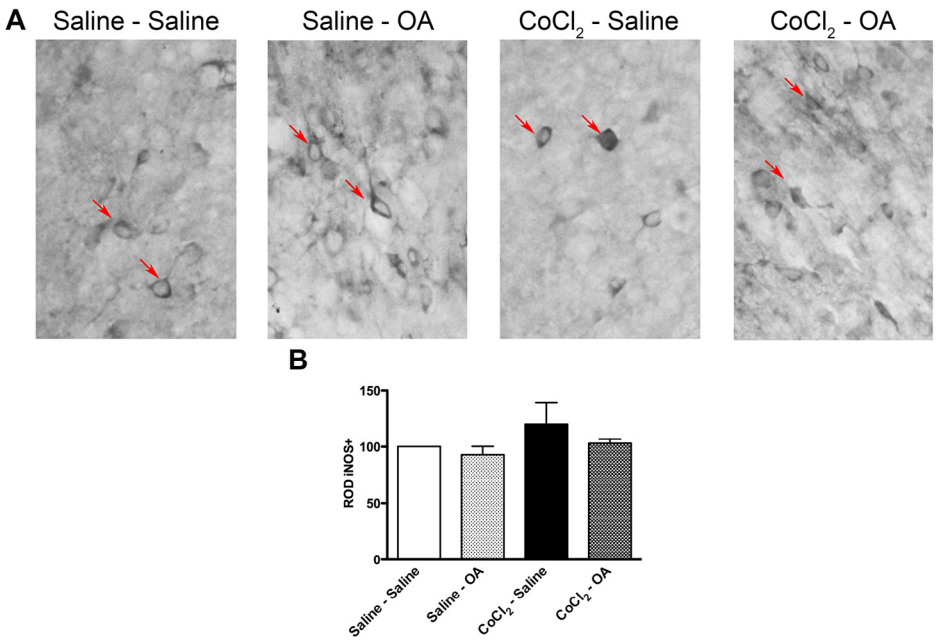

Fig. 9. A. Fotomicrography of iNOS immunostaining. Primary magnification 20×. B. ROD of iNOS. Significance between treatments after one-way ANOVA and Tukey's post-test. Red arrows show iNOS+ cells.

Over 300 synthetic derivatives of OA have been generated and tested for their ability to inhibit oxidant stress and nitric oxide production in activated macrophages by abrogating the synthesis of iNOS and cyclooxygenase 2 (Honda et al., 2002). The mechanisms involved in the role of triterpenoid compounds include decreasing the levels of reactive oxygen species (ROS) through the activation of Nrf2-dependent transcription of anti-oxidant and detoxification genes (Dinkova-Kostova et al., 2005; Thimmulappa et al., 2006). In our study, iNOS optical density increased after $CoCl_2$ injection and showed a decreasing tendency in the OA-pre-treated group, in accordance with the inhibition of the nitrergic system in microglia.

In previous reports (Caltana et al., 2009), the hypoxic model induced by the intracortical injection of $CoCl_2$ produced focal hypoxic injury within the brain cortex. Here we report that OA is capable of protecting cortical neurons when administered before and after brain hypoxic conditions. In particular, OA was able to increase neuronal survival, improve dendrite recovery and reduce astroglial and microglial reaction. In line with our results, the ability of natural OA and its synthetic analogs to modulate microglial, astrocytic and neuronal activities, thus providing neuroprotection against inflammatory damage, has also been described in *in vitro* and *in vivo* models of neurodegenerative diseases, including multiple sclerosis and Alzheimer's (Dumont et al., 2009; Graber et al., 2011; Martin et al., 2012; Tran et al., 2008).

With these results, and considering that neuronal damage activates astroglial and microglial response, which interfere with neuronal recovery, we hypothesize that the pre-treatment with OA might act as a neuroprotective agent, reducing both neuronal damage and glial reaction, and hence taking part in nervous tissue recovery after injury.

Acknowledgments

We thank Mrs. Emerita Jorge Vilela de Bianchieri for her technical assistance. This study is supported by grants UBACYT 000093 (A.B.)

References

Balan, I.S., Fiskum, G., Hazelton, J., Cotto-Cumba, C., Rosenthal, R.E., 2006. Oximetry-guided reoxygenation improves neurological outcome after experimental cardiac arrest. Stroke 37 (12), 3008–3013.
Bao, X., Gao, M., Xu, H., Liu, K.X., Zhang, C.H., Jiang, N., et al., 2014. A novel oleanolic acid-loaded PLGA-TPGS nanoparticle for liver cancer treatment. Drug Dev. Ind. Pharm. doi:10.3109/03639045.2014.938081 (in press).
Berra, E., Ginouvès, A., Pouysségur, J., 2006. The hypoxia-inducible-factor hydroxylases bring fresh air into hypoxia signalling. EMBO Rep. 7, 41–45.
Caltana, L., Merelli, A., Lazarowski, A., Brusco, A., 2009. Neuronal and glial alterations due to focal cortical hypoxia induced by direct cobalt chloride ($CoCl_2$) brain injection. Neurotox. Res. 15, 348–358.
Chiva-Blanch, G., Badimon, L., Estruch, R., 2014. Latest evidence of the effects of the Mediterranean diet in prevention of cardiovascular disease. Curr. Atheroscler. Rep. doi:10.1007/s11883-014-0446-9 (in press).
Delgado-Lista, J., Perez-Martinez, P., Garcia-Rios, A., Perez-Caballero, A.I., Perez-Jimenez, F., Lopez-Miranda, J., 2014. Mediterranean diet and cardiovascular risk: beyond traditional risk factors. Crit. Rev. Food Sci. Nutr. doi:10.1080/10408398.2012.726660 (in press).
Dinkova-Kostova, A.T., Liby, K.T., Stephenson, K.K., Holtzclaw, W.D., Gao, X., Suh, N., et al., 2005. Extremely potent triterpenoid inducers of the phase 2 response: correlations of protection against oxidant and inflammatory stress. Proc. Natl Acad. Sci. U.S.A. 102, 4584–4589.
Dumont, M., Wille, E., Calingasan, N.Y., Tampellini, D., Williams, C., Gouras, G.K., et al., 2009. Triterpenoid CDDO-methylamide improves memory and decreases amyloid plaques in a transgenic mouse model of Alzheimer's disease. J. Neurochem. 109, 502–512.
Epstein, A.C., Gleadle, J.M., McNeill, L.A., Hewitson, K.S., O'Rourke, J., Mole, D.R., et al. 2001. C. elegans EGL-9 and mammalian homologs define a family of dioxygenases that regulate HIF by prolyl hydroxylation. Cell. 107 (1), 43–54.
Evrard, S., Duhalde-Vega, M., Tagliaferro, P., Mirochnic, S., Caltana, L., Brusco, A., 2006. A low chronic ethanol exposure induces morphological changes in the adolescent rat brain that are not fully recovered even after a long abstinence: an immunohistochemical study. Exp. Neurol. 200 (2), 438–459.
Fontanay, S., Grare, M., Mayer, J., Finance, C., Duval, R.E., 2008. Ursolic, oleanolic and betulinic acids: antibacterial spectra and selectivity indexes. J. Ethnopharmacol. 120, 272–276.
Graber, D.J., Park, P.J., Hickey, W.F., Harris, B.T., 2011. Synthetic triterpenoid CDDO derivatives modulate cytoprotective or immunological properties in astrocytes, neurons, and microglia. J. Neuroimmune Pharmacol. 6, 107–120.
Honda, T., Honda, Y., Favaloro, F.G., Jr., Gribble, G.W., Suh, N., Place, A.E., et al., 2002. A novel dicyanotriterpenoid, 2-cyano-3,12-dioxooleana-1,9(11)-dien-28-onitrile, active at picomolar concentrations for inhibition of nitric oxide production. Bioorg. Med. Chem. Lett. 12 (7), 1027–1030.

Hu, J., Van Eldik, L.J., 1996. S100β induces apoptotic cell death in cultured astrocytes via a nitric oxide-dependent pathway. Biochim. Biophys. Acta 1313, 239–245.
Hu, J., Ferreira, A., Van Eldik, L.J., 1997. S100β induces neuronal cell death through nitric oxide release from astrocytes. J. Neurochem. 69, 2294–2301.
Hunan Med. Inst., 1977. Effects of oleanolic acid on experimental liver injury and therapeutic value in human hepatitis. Tradit. Med. (Zhong Chao Yao) 8, 32–37.
Ignácio, A.R., Muller, Y.M.R., Carvalho, M.S.L., Nazari, E.M., 2005. Distribution of microglial cells in the cerebral hemispheres of embryonic and neonatal chicks. Braz. J. Med. Biol. Res. 38, 1615–1622.
Janahmadi, Z., Nekooeian, A.A., Moaref, A.R., Emamghoreishi, M., 2014. Oleuropein offers cardioprotection in rats with acute myocardial infarction. Cardiovasc. Toxicol. doi:10.1007/s12012-014-9271-1 (in press).
Karovic, O., Tonazzini, I., Rebola, N., Edström, E., Lövdahl, C., Fredholm, B.B., et al., 2007. Toxic effects of cobalt in primary cultures of mouse astrocytes: similarities with hypoxia and role of HIF-1 alpha. Biochem. Pharmacol. 73, 694–708.
Kunz, A., Dirnagl, U., Mergenthaler, P., 2010. Acute pathophysiological processes after ischaemic and traumatic brain injury. Best Prac. Res. Clin. Anaesthesiol. 24, 495–509.
Lee, W., Yang, E.J., Ku, S.K., Song, K.S., Bae, J.S., 2013. Anti-inflammatory effects of oleanolic acid on LPS-induced inflammation in vitro and in vivo. Inflammation 36 (1), 94–102.
Lloyd-Jones, D., Adams, R., Brown, T., Carnethon, M., Dai, S., De Simone, G., et al., 2010. Heart disease and stroke statistics. 2010 Update: A Report From the American Heart Association. Circulation 121, e46–e215.
Mackay, J., Mensah, G., 2004. WHO publishes definitive atlas on global heart disease and stroke epidemic. Indian J. Med. Sci. 58 (9), 405–406.
Martin, R., Hernandez, M., Cordova, C., Nieto, M., 2012. Natural triterpenes modulate immune-inflammatory markers of experimental autoimmune encephalomyelitis: therapeutic implications for multiple sclerosis. Br. J. Pharmacol. 166 (5), 1708–1723.
Moro, M.A., Cárdenas, A., Hurtado, O., Leza, J.C., Lizasoain, I., 2004. Role of nitric oxide after brain ischaemia. Cell Calcium 36 (3–4), 265–275.
Nardin, P., Tramontina, F., Leite, M.C., Tramontina, A.C., Quincozes-Santos, A., de Almeida, L.M., et al., 2007. S100b content and secretion decrease in astrocytes cultured in high-glucose medium. Neurochem. Int. 50 (5), 774–782.
Paxinos, G., Watson, C., 2013. The rat brain in stereotaxic coordinates, seventh ed. Academic Press, San Diego.
Ramos, A.J., Rubio, M.D., Defagot, C., Hischberg, L., Villar, M.J., Brusco, A., 2004. The 5HT1A receptor agonist, 8-OH-DPAT, protects neurons and reduces astroglial reaction after ischemic damage caused by cortical devascularization. Brain Res. 1030 (2), 201–220.
Ratan, R.R., Siddiq, A., Smirnova, N., Karpisheva, K., Haskew-Layton, R., McConoughey, S., et al., 2007. Harnessing hypoxic adaptation to prevent, treat, and repair stroke. J. Mol. Med. 85, 1331–1338.
Rodriguez, J.A., Astudillo, L., Schmeda-Hirschmann, G., 2003. Oleanolic acid promotes healing of acetic acid-induced chronic gastric lesions in rats. Pharmacol. Res. 48, 291–294.
Rong, Z.T., Gong, X.J., Sun, H.B., Li, Y.M., Ji, H., 2011. Protective effects of oleanolic acid on cerebral ischemic damage in vivo and H(2)O(2)-induced injury in vitro. Pharm. Biol. 49, 78–85.
Sarkar, C., Pal, S., Das, N., Dinda, B., 2014. Ameliorative effects of oleanolic acid on fluoride induced metabolic and oxidative dysfunctions in rat brain: experimental and biochemical studies. Food Chem. Toxicol. 66, 224–236.
Scherer-Singler, U., Vincent, S.R., Kimura, H., McGeer, E.G., 1983. Demonstration of a unique population of neurons with NADPH-diaphorase histochemistry. J. Neurosci. Methods 9, 229–234.
Selinfreund, R.H., Barger, S.W., Pledger, W.J., Van Eldik, L.J., 1991. Neurotrophic protein S100β stimulates glial cell proliferation. Proc. Natl Acad. Sci. U.S.A. 88, 3554–3558.
Singh, G.B., Singh, S., Bani, S., Gupta, B.D., Banerjee, S.K., 1992. Anti-inflammatory activity of oleanolic acid in rats and mice. J. Pharm. Pharmacol. 44, 456–458.
Srivastava, P., Kasoju, N., Bora, U., Chaturvedi, R., 2010. Accumulation of betulinic, oleanolic, and ursolic acids in in vitro cell cultures of Lantana camara L. and their significant cytotoxic effects on HeLa cell lines. Biotechnol. Bioprocess Eng. 15, 1038–1046.
Sultana, N., Saify, Z.S., 2012. Naturally occurring and synthetic agents as potential anti-inflammatory and immunomodulants. Antiinflamm Antiallergy Agents Med. Chem. 11 (1), 3–19.
Thimmulappa, R.K., Scollick, C., Traore, K., Yates, M., Trush, M.A., Liby, K.T., et al., 2006. Nrf2-dependent protection from LPS induced inflammatory response and mortality by CDDO-Imidazolide. Biochem. Biophys. Res. Commun. 351, 883–889.
Tramontina, F., Tramontina, A.C., Souza, D.F., Leite, M.C., Gottfried, C., Souza, D.O., et al., 2006. Glutamate uptake is stimulated by extracellular S100b in hippocampal astrocytes. Cell. Mol. Neurobiol. 26, 81–86.
Tran, T.A., McCoy, M.K., Sporn, M.B., Tansey, M.G., 2008. The synthetic triterpenoid CDDO-methyl ester modulates microglial activities, inhibits TNF production, and provides dopaminergic neuroprotection. J. Neuroinflammation 5, 14.
Tsai, S.J., Yin, M.C., 2012. Anti-oxidative, anti-glycative and anti-apoptotic effects of oleanolic acid in brain of mice treated by D-galactose. Eur. J. Pharmacol. 689 (1–3), 81–88.
Villar, V.H., Vögler, O., Barceló, F., Gómez-Florit, M., Martínez-Serra, J., Obrador-Hevia, A., et al., 2014. Oleanolic and maslinic acid sensitize soft tissue sarcoma cells to doxorubicin by inhibiting the multidrug resistance protein MRP-1, but not P-glycoprotein. J. Nutr. Biochem. 25 (4), 429–438.
Yuan, Y., Hilliard, G., Ferguson, T., Millhorn, D.E., 2003. Cobalt inhibits the interaction between hypoxia-inducible factor-alpha and von Hippel-Lindau protein by direct binding to hypoxia-inducible factor-alpha. J. Biol. Chem. 278, 15911–15916.
Zhang, F., Wang, S., Zhang, M., Wenq, Z., Li, P., Gan, Y., et al., 2012. Pharmacological induction of heme oxygenase-1 by a triterpenoid protects neurons against ischemic injury. Stroke 43 (5), 1390–1397.